

Brain Structural Changes in Obstructive Sleep Apnea

Paul M. Macey, PhD^{1,2}; Rajesh Kumar, PhD³; Mary A. Woo, DNSc²; Edwin M. Valladares, BS³; Frisca L. Yan-Go, MD⁴; Ronald M. Harper, PhD^{1,3}

¹Brain Research Institute, ²UCLA School of Nursing, Departments of ³Neurobiology and ⁴Neurology, David Geffen School of Medicine at UCLA, University of California Los Angeles, Los Angeles, CA

Study Objectives: Determine whether obstructive sleep apnea (OSA) subjects show indications of axonal injury.

Design: We assessed fiber integrity in OSA and control subjects with diffusion tensor imaging (DTI). We acquired four whole-brain DTI series from each subject. The four series were realigned, and the diffusion tensor calculated at each voxel. Fractional anisotropy (FA), a measure of fiber integrity, was derived from the diffusion tensor, resulting in a whole brain FA “map.” The FA maps were spatially normalized, smoothed, and compared using voxel-based statistics to determine differences between OSA and control groups, with age as a covariate ($P < 0.05$, corrected for multiple comparisons).

Setting: University medical center.

Subjects: We studied 41 patients with untreated OSA (mean age \pm SD: 46.3 \pm 8.9 years; female/male: 7/34) with apnea-hypopnea index 15 to 101 (mean \pm SD: 35.7 \pm 18.1 events/hour), and 69 control subjects (mean age \pm SD: 47.5 \pm 8.79 years; female/male: 25/44).

Measurements and Results: Multiple regions of lower FA appeared within white matter in the OSA group, and included fibers of the anterior corpus callosum, anterior and posterior cingulate cortex and cingulum bundle, right column of the fornix, portions of the frontal, ventral prefrontal, parietal and insular cortices, bilateral internal capsule, left cerebellar peduncle, middle cerebellar peduncle and corticospinal tract, and deep cerebellar nuclei.

Conclusions: White matter is extensively affected in OSA patients; the alterations include axons linking major structures within the limbic system, pons, frontal, temporal and parietal cortices, and projections to and from the cerebellum.

Keywords: Magnetic resonance imaging, fractional anisotropy, diffusion tensor imaging, hypoxia, cingulate cortex

Citation: Macey PM; Kumar R; Woo MA; Valladares EM; Yan-Go FL; Harper RM. Brain structural changes in obstructive sleep apnea. *SLEEP* 2008;31(7):967-977.

OBSTRUCTIVE SLEEP APNEA (OSA) IS ACCOMPANIED BY AFFECTIVE, COGNITIVE, AND AUTONOMIC NERVOUS SYSTEM CHANGES¹⁻⁴ THAT SUGGEST CENTRAL nervous systems alterations in brain regions mediating these behaviors. Retention of cognitive and mood problems, despite treatment,⁵⁻⁷ as well as sustained elevated sympathetic outflow⁸ and impaired autonomic responses to transient challenges⁹⁻¹¹ indicate that disturbed neural functions account for at least some of the characteristics accompanying OSA. Altered neural function is found in response to a number of cognitive, respiratory and autonomic challenges using functional magnetic resonance imaging (fMRI).^{7,9-13} The functional alterations of the brain in OSA likely result, at least in part, from injury to neural structures, but the nature of such injury is not fully understood.

Cerebral damage is not obvious on routine magnetic resonance imaging (MRI) examination in OSA subjects,¹⁴ but more sensitive anatomical MRI techniques reveal structural changes in brain regions that also show functional alterations, including areas which regulate memory and planning functions and affect (e.g., anterior cingulate, hippocampus, and frontal cortical regions), and in areas underlying regulation of autonomic outflow (e.g., anterior cingulate, cerebellar, and brainstem areas).¹⁵⁻²⁰

Disclosure Statement

This was not an industry supported study. The authors have indicated no financial conflicts of interest.

Submitted for publication November, 2007

Accepted for publication February, 2008

Address correspondence to: Ronald M. Harper, PhD, Department of Neurobiology, David Geffen School of Medicine at UCLA, University of California at Los Angeles, Los Angeles, CA 90095-1763; Tel: (310) 825-5303; Fax: (310) 825-2224; E-mail: rharper@ucla.edu

Magnetic resonance spectroscopy studies of isolated brain regions (i.e., manually selected voxels) consistently show signs of reduced neuronal density or altered metabolism in OSA groups, but these studies are limited in the brain structures studied (hippocampus, parietal-occipital white matter and cortex), and are constrained by the poor spatial resolution of the technique.¹⁷⁻²⁰ Regional gray matter volume, which decreases with atrophy and cell death, can be evaluated with high-resolution anatomical images across the whole brain; we earlier showed a number of brain areas with lower volume, including many overlapping functionally-affected regions.¹⁵ However, these findings were subsequently replicated only partially¹⁶ or not at all,²¹ likely a consequence of differences in analysis methodology (including higher statistical thresholds) and of subject variation.²² Human studies of brain structure to date offer some evidence of injury or atrophy, but do not fully explain the extent of central nervous system functional changes found in OSA.

A portion of the impaired autonomic, cognitive, or emotional functions in OSA may develop from alterations to projecting fibers between affected structures. The fiber changes may develop as a consequence of cellular damage, resulting from ischemic, hypoxic, or inflammatory processes accompanying the sleep disordered breathing. Attempts to mimic OSA characteristics in animal models, such as imposition of repeated intermittent hypoxia, result in neuronal injury in brain regions similar to those areas affected in the human syndrome, as well as damage to axons within both white matter tracts and nerve fibers within the gray matter.²³⁻²⁶ In OSA subjects, discrete brain regions (hippocampus, parietal white matter) show alterations in metabolite levels indicative of axonal loss or injury.^{18,20} Axonal changes are not necessarily as extreme as the cell death or shrinkage associated with atrophy, since axons may undergo diameter reduction and lose much of their myelin sheath without

Table 1—Characteristics of OSA and Control Subjects

	OSA N = 41		CONTROL N = 69		OSA vs CONTROL P
	Mean ± SD	Range	Mean ± SD	Range	
AHI	35.7 ± 18.1	15–100	n/a		
SpO ₂ * (minimum)	79.8% ± 9.5%	50–96			
SpO ₂ * (baseline)	94.8% ± 2.1%	88–97			
Age (years)	46.3 ± 8.9	30–61	47.5 ± 8.9	30–65	0.5
BMI	30.5 ± 4.8	21.5–43.2	25.3 ± 4.8	16.6–38.1	< 0.001
Sex	7♀, 34♂		25♀, 44♂		0.03
Hypertension	11 (27%)		5 (7%)		0.01
Diabetes (Type 2)	4 (10%)		0		0
Prior History of Smoking	5 (12%)		5 (7%)		0.5
Prior History of Cardiovascular Medication †	6 (15%)		2 (3%)		0.02
Prior History of Antidepressant	3 (7%)		0		
Epworth ‡	9.8 ± 4.5	0–19	5.5 ± 3.3	0–14	< 0.001
PSQI §	9.6 ± 4.3	0–20	4.0 ± 2.5	0–12	< 0.001

* One subject omitted due to signal artifact

† Inhibitors of Angiotensin-Converting Enzyme, Angiotensin II Receptor Blocker

‡ Epworth Sleepiness Scale; ≥ 9 indicates excessive sleepiness

§ Pittsburg Sleep Quality Index; > 5 indicates poor sleep quality

axonal death, an effect found in animal models of intermittent hypoxia.^{24,27} Such axonal alterations, if present, would interfere with communication between brain structures, and thus modify function of those structures.

Newer MRI modalities allow more accurate examination of fiber integrity. Diffusion tensor imaging (DTI) is sensitive to the microstructure of brain tissue²⁸; various indices can be derived from DTI data, including fractional anisotropy (FA), which is sensitive to the number, coherence, and degree of myelination of fibers.²⁹ Whole-brain voxel-based analysis of FA, akin to voxel-based morphometry used in gray matter volume studies, can highlight axonal changes both in major fiber tracts and in other parallel groups of axons bordering the tracts or extending into cellular areas.³⁰ The voxel-based approach is suitable for detecting regions of consistent difference between groups, and could locate brain areas that are affected within an OSA group relative to a control population.

We hypothesized that OSA is accompanied by significant alterations in axons, and that these changes will be reflected as significantly lower FA in a group of OSA patients relative to control subjects, as assessed with voxel-based analyses. We expected structural changes in white matter tracts linking brain areas that show functional changes, in particular limbic areas (especially, the hippocampus, insula and anterior cingulate), the cerebellum, and cognitive areas in the frontal cortex. To address the small size and possible heterogeneity of samples in earlier studies, we aimed to study a larger set of subjects with more clearly-defined inclusion and exclusion criteria, and minimize confounding factors that could affect neuronal alterations.

METHODS

Subjects

Our target sample was a minimum of 83 subjects with at least 40 per group, as determined by a power analysis.³¹ We assumed

a large effect size (Cohen's *f* of 0.4), and aimed to control for an error probability (α) of 0.05 and a false negative rate (β) of 0.1 (i.e., power of 0.9), based on a 2-group ANOVA with one covariate (age). We targeted moderate and severe OSA patients (apnea-hypopnea index [AHI] ≥ 15), and the OSA and control groups were approximately matched by age and sex distributions. Control and OSA subjects were recruited simultaneously until at least 40 OSA subjects had completed the study (and met inclusion criteria), after which additional control subjects were recruited to attempt to ensure the groups were matched for age and sex; we used more than the minimum number of control subjects to improve statistical power.

Obstructive sleep apnea subjects were recruited through the UCLA Sleep Disorders Laboratory, and control subjects through flyers in the university medical center. No subjects showed a history of major mental disorder, brain injury or illness, cerebrovascular disease, or major cardiovascular disorder (e.g., stroke, heart failure, myocardial infarction). All subjects were free of mood-altering or cardiovascular medications. Subjects with visible brain pathology (e.g., benign cyst, evidence of traumatic brain injury) were excluded. Exclusion criteria related to scanner limitations for all subjects also included weight > 125 kg, claustrophobia, and upper body metallic implants or devices.

All OSA patients underwent an overnight polysomnography study at the UCLA Sleep Disorders Laboratory, and were scored and classified according to standard criteria by Laboratory personnel.³² Patients included in the study were diagnosed as having moderate-to-severe OSA (AHI of 15 to 101; see Table 1). All patients were untreated for OSA, i.e., most were recently diagnosed, and none had experienced continuous positive airway pressure (CPAP) or other intervention.

Control subjects were assessed by an interview with the subject and cosleeper, when available, to ensure absence of sleep disordered breathing. Four subjects initially enrolled as controls who showed signs of potential OSA were studied using over-

night polysomnography; one subject was reassigned to the OSA group, two subjects were confirmed as controls (AHI < 5), and one subject was diagnosed with mild OSA and excluded (the final numbers of subjects are in Table 1). Two control subjects who showed signs of respiratory disturbance during scanning, namely periodic breathing, were also excluded.

Participants provided written consent, and the study was approved by the Institutional Review Board at UCLA.

Sleep Questionnaires

To further characterize the sample, we assessed factors associated with OSA, namely daytime sleepiness with the Epworth Sleepiness Scale (ESS) and sleep quality with the Pittsburgh Sleep Quality Index (PSQI). These self-administered questionnaires were completed by subjects after the MRI scanning protocol. Both measures are commonly used indices of sleepiness and sleep quality.³³

MRI Protocol

Using a 3.0-Tesla MRI scanner (Siemens Trio with 8-channel head coil), four whole-brain DTI series were acquired. Diffusion tensor imaging was performed using a single-shot multi-section spin-echo echo-planar pulse sequence (repetition time [TR] = 10,000 ms; echo-time [TE] = 87 ms; flip angle = 90°) in the axial plane, with a 128 × 128 matrix size, 230 × 230 mm field of view (FOV), 2.0 mm slice thickness, 75 slices and no interslice gap, and a readout bandwidth of 1346 Hz/pixel. For each slice, diffusion gradients were applied along 12 independent orientations with $b = 700 \text{ s/mm}^2$ after the acquisition of $b = 0 \text{ s/mm}^2$ (b_0) images. An acceleration factor of two was applied using the parallel imaging generalized-autocalibrating-partially-parallel-acquisition technique. To enable correction for field-related distortions, we collected phase-difference and magnitude images (1st TE = 4.98 ms, 2nd TE = 7.44 ms; TR = 880 ms; flip angle = 90°; matrix size = 64 × 64; FOV = 192 × 192 mm; slice thickness = 3.0 mm; number of slices = 36). High-resolution three-dimensional T1-weighted anatomical scans were also collected using a magnetization-prepared-rapid-acquisition-gradient-echo pulse sequence (TR = 2200 ms; TE = 2.2 ms; inversion time = 900 ms; flip angle = 9°; matrix size = 256 × 256; FOV = 230 × 230 mm; slice thickness = 1.0 mm; number of slices = 176) for evaluation of any anatomical defects. Scans were visually verified as free from significant movement or other artifact at the time of scanning; if problems were identified, scans were repeated. The data were processed using SPM5 (www.fil.ion.ucl.ac.uk/spm/) and custom routines in Matlab (The MathWorks Inc., MA).

Analysis

The three later series were realigned to the first series' b_0 image using the non-diffusion weighted (b_0) images; the direction vectors of the realigned diffusion-weighted images were rotated accordingly. Phase distortions due to magnetic field inhomogeneities were corrected using fieldmaps calculated from the phase-difference and magnitude images, with software from the SPM5 "Fieldmap" toolbox.³⁴ The diffusion

tensor, a numerical representation of the directional diffusion properties, was calculated at each voxel using a linear regression model, with an additional constant term for each direction to allow for direction-depending global signal intensity variations.³⁵ Fractional anisotropy (FA), a measure of fiber integrity,^{29,36} was derived from the tensor at each voxel, resulting in a whole brain FA "map." The spatial normalization of the mean of the four b_0 images to the Montreal Neurological Institute (MNI) T2-weighted template was used to spatially normalize the FA maps, using the unified bias correction, tissue segmentation and spatial normalization procedure included with the SPM5 software.³⁷ The spatial normalization consisted of a 12-parameter affine transformation followed by a nonlinear warping defined by $7 \times 8 \times 7$ cosine basis functions (x, y, z directions). The normalized FA maps were smoothed (full-width-half-maximum = 10 mm). The choice of smoothing kernel can exert a significant effect upon the results,³⁸ we considered 10 mm to be sufficiently large to account for variance in the anatomy of the spatially normalized images, and sufficiently small to highlight expected differences in fiber. Smoothed FA maps were compared using voxel-based statistics for differences between OSA and control groups using ANCOVA, with age as a covariate (threshold $P < 0.05$, corrected for multiple comparisons using false discovery rate). Clusters of significant FA differences were overlaid onto a spatially normalized T1-weighted anatomical image, the MNI reference brain.

Selected clusters were overlaid onto a background indicating fiber direction. The principal direction of diffusion can be visualized by combining the $x, y,$ and z components of the first eigenvector of a diffusion tensor as red, green, and blue components of a true color image, scaled by FA.³⁹ To reorient the tensor directions into the template space, the preservation of principal directions method was used,⁴⁰ and each of the $x, y,$ and z components were averaged over all subjects, highlighting locations of major fiber tracts.

Subject characteristics were compared between groups using independent t-tests for continuous variables and Chi-square tests for categorical variables.

RESULTS

Subjects

A total of 41 OSA patients and 69 control subjects participated (see Table 1). The groups were matched by age, but there was a significant difference between the OSA and control sex distributions, due to subject exclusion after treatment. As expected, the OSA patients had a higher body mass index (BMI) than the control subjects. Hypertension was significantly more frequent in the OSA group (27% versus 7%), and type 2 diabetes mellitus was present in 10% of the OSA patients, but none of the control subjects. Although our exclusion criteria included no history of major cardiovascular disease or mental illness, small numbers of subjects reported prior use of cardiovascular medications and antidepressants (significantly more in the OSA group). Five subjects from each group had a prior history of smoking.

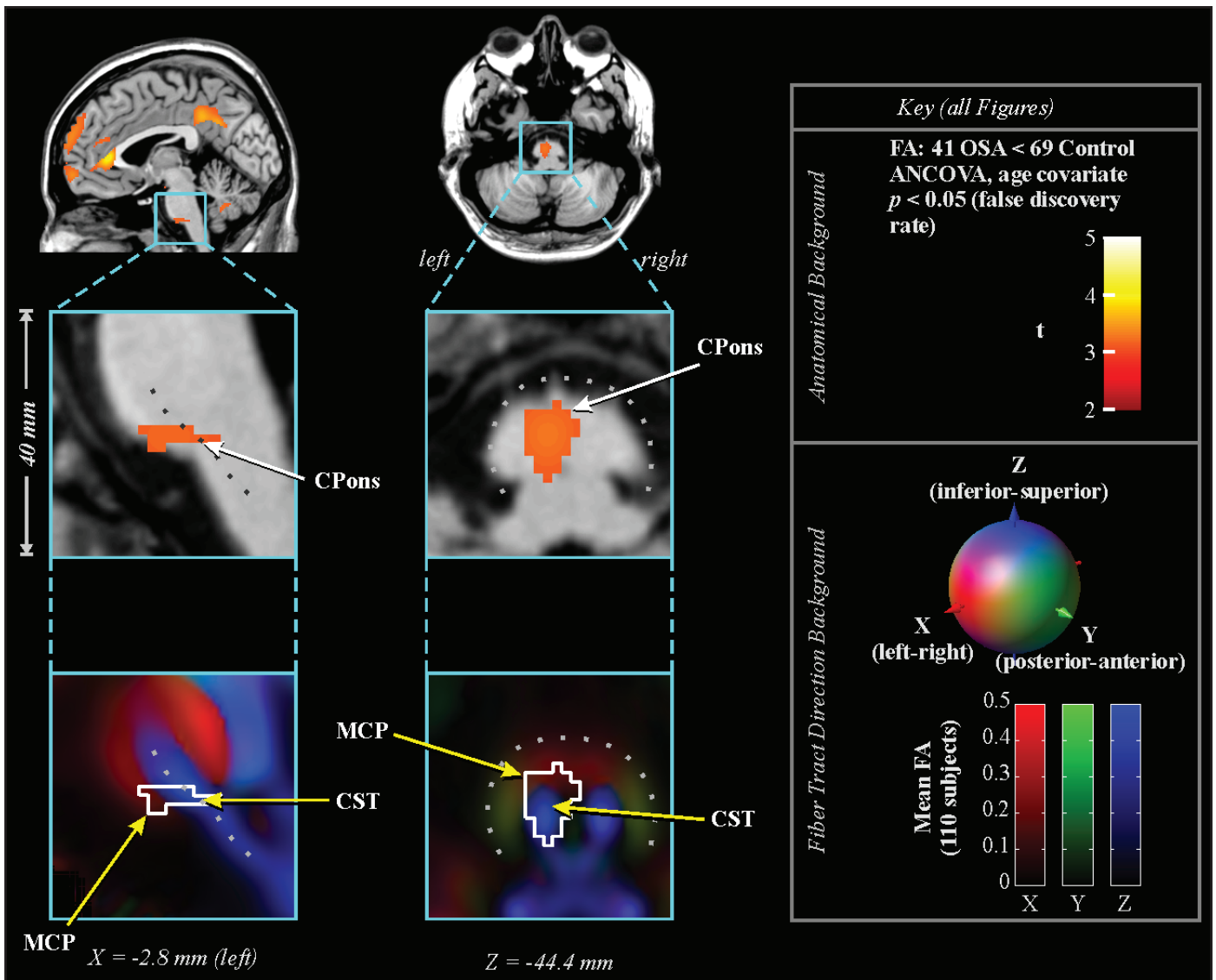


Figure 1—Lower FA in 41 OSA vs 69 control subjects. Top: regions overlaid on single subject's anatomical background in sagittal (left) and axial (right) views, color coded according to significance (key at right), with close-up of caudal pons below. Bottom: same regions outlined on background indicating fiber tract direction (average of 110 subjects; directions indicated by lower color key). Locations are in MNI space (relative to anterior commissure). CPons: caudal pons; MCP: middle cerebellar peduncle; CST: corticospinal tract.

Neural Alterations: Lower FA in OSA

Lower FA values in OSA, compared with control subjects, appeared in multiple brain areas (listed in Table 2), and no regions showed greater FA in OSA over control subjects; age effects were controlled by inclusion of an age covariate.

The caudal pons showed lower FA in the OSA group in a region containing cellular groups, the left middle cerebellar peduncle, and the left corticospinal tract (Figure 1). The deep cerebellar nuclei were affected (Figure 2A), as was the ventral lateral thalamus extending to the temporal cortex in regions adjacent to the amygdala and hippocampus (Figure 2B); a small portion of the right column of the fornix showed lower FA (Figure 2C). Reduced integrity appeared in the left cerebral peduncle, within a medial region of the cerebral crus containing fibers from upper body areas (Figure 3). A large area in the anterior cingulate gyrus showed lower FA, and included the cingulate cortex and cingulum bundle; an adjacent region of the corpus callosum was

affected (Figure 4). An area of the posterior cingulum bundle and surrounding posterior cingulate cortex also showed reduced FA (Figure 5A). White matter near the pole of the temporal lobe, in the inferior longitudinal fasciculus, was affected (Figure 5B). The bilateral internal capsule showed reduced integrity, as did white matter adjacent to the left anterior and right mid-insula (Figure 5C). Finally, regions in the parietal and frontal cortices showed lower FA, especially bilaterally in medial prefrontal areas and in ventral medial frontal cortex (Figure 6).

DISCUSSION

Overview

White matter is extensively altered in OSA patients. The affected regions include the internal capsule and ventral lateral thalamus with axonal connections to the nearby hippocampus and amygdala, and to the cerebral peduncle. Structural changes also

Table 2—All Distinct Regions (Clusters) of Lower FA in 41 OSA vs 69 Control Subjects. Location of Maximum Effect is Shown in Montreal Neurological Institute (MNI) Space (mm from Anterior Commissure). Group Mean Values Across All Voxels in Each Cluster are Shown, With Between-Subject Standard Deviations. Some Clusters Encompass Multiple Regions.

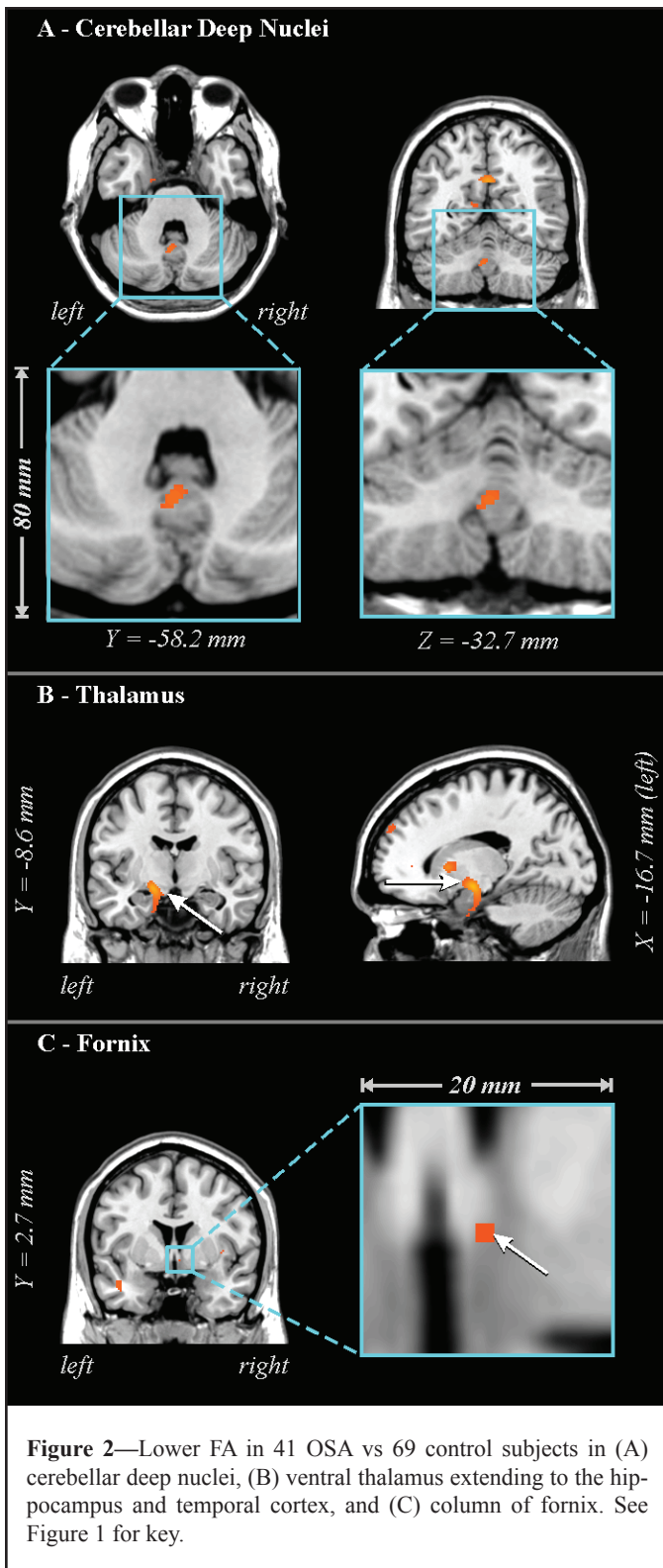
Location	MNI coordinates			Voxels 3.4 mm ³	Control Mean ± SE	OSA	
	X	Y	Z			Mean ± SE	Figure
Cerebellum/brainstem							
caudal pons/middle cerebellar peduncles, corticospinal tract cerebellum	-3	-23	-45	70	0.2967 ± 0.0057	0.2669 ± 0.0068	Figure 1
	-3	-59	-35	52	0.2531 ± 0.0025	0.2407 ± 0.0025	Figure 2A
Thalamus/midbrain/regions adjacent to hippocampus							
ventral lateral thalamus adjacent to amygdala and hippocampus midbrain	-17	-8	-11	409	0.3721 ± 0.0035	0.3585 ± 0.0057	Figure 2B Figure 3
right fornix column	+5	+3	-5	2	0.2429 ± 0.0034	0.2340 ± 0.0044	Figure 2C
Cingulate cortex/cingulum							
inferior longitudinal fasciculus	-44	+2	-24	124	0.2222 ± 0.0025	0.2083 ± 0.0028	Figure 5B
anterior cingulate cortex/superior cingulum, corpus callosum genu, cingulum	-9	+39	-9	2732	0.2537 ± 0.0038	0.2221 ± 0.0030	Figure 4
	8.3	38	9.7				
Posterior inferior-cingulum	+24	-39	-5	9	0.2795 ± 0.0059	0.2537 ± 0.0044	Figure 5A
inferior fronto-occipital fasciculus	-38	-27	0	57	0.3386 ± 0.0032	0.3237 ± 0.0047	Figure 5C
posterior cingulate gyrus	-9	-57	+14	40	0.2494 ± 0.0065	0.2123 ± 0.0057	Figure 5A
posterior cingulate cortex	+3	-53	+32	1517	0.2368 ± 0.0043	0.2089 ± 0.0047	Figure 5A
Deep white matter, insula							
right internal capsule	+23	-2	+2	22	0.3579 ± 0.0041	0.3330 ± 0.0047	Figure 5C
left anterior internal capsule	-17	+15	+3	124	0.3446 ± 0.0036	0.3263 ± 0.0054	Figure 5C
right anterior internal capsule	+17	+15	+3	38	0.3164 ± 0.0037	0.2984 ± 0.0063	Figure 5C
posterior internal capsule	-38	-39	+15	10	0.3965 ± 0.0039	0.3757 ± 0.0061	
left anterior insula	-36	+17	+2	104	0.1997 ± 0.0021	0.1875 ± 0.0027	Figure 5C
right mid insula	+39	+5	+2	7	0.1975 ± 0.0027	0.1838 ± 0.0026	Figure 5C
Frontal and Prefrontal							
left lateral prefrontal	-44	+44	-9	136	0.2182 ± 0.0032	0.1963 ± 0.0039	Figure 6
ventral medial prefrontal	+2	+36	-24	7	0.1482 ± 0.0033	0.1283 ± 0.0032	Figure 6
ventral lateral prefrontal	-29	+18	-24	13	0.1580 ± 0.0044	0.1356 ± 0.0033	Figure 6
medial prefrontal	-8	+59	-11	3	0.2060 ± 0.0074	0.1715 ± 0.0036	Figure 6
right prefrontal	+30	+60	+8	267	0.2223 ± 0.0063	0.1867 ± 0.0040	Figure 6
left medial frontal	-3	+69	+18	1766	0.1697 ± 0.0100	0.1161 ± 0.0040	Figure 6
right lateral frontal	+41	+35	+12	2	0.3236 ± 0.0044	0.2993 ± 0.0047	Figure 6
right frontal	+26	+62	+30	134	0.1335 ± 0.0065	0.0991 ± 0.0040	Figure 6
left lateral frontal	-45	+27	+26	13	0.2823 ± 0.0047	0.2024 ± 0.0046	Figure 6
left deep frontal	-23	+29	+44	4	0.2291 ± 0.0046	0.2059 ± 0.0048	Figure 6
left lateral frontal	-51	+8	+12	26	0.2104 ± 0.0042	0.1876 ± 0.0032	Figure 6
Parietal							
right postcentral sulcus	+32	-29	+56	39	0.2633 ± 0.0034	0.2464 ± 0.0042	Figure 6
precentral gyrus	+5	-24	+63	22	0.2394 ± 0.0055	0.2100 ± 0.0060	Figure 6
left central gyrus	-21	-12	+69	4	0.2088 ± 0.0040	0.1917 ± 0.0043	
left deep lateral parietal	-51	-50	+5	2	0.2660 ± 0.0048	0.2424 ± 0.0052	
left parietal operculum	-45	-18	+15	117	0.1960 ± 0.0031	0.1293 ± 0.0025	Figure 5B
Temporal							
superior longitudinal fasciculus	+42	-20	+5	2	0.2450 ± 0.0029	0.2299 ± 0.0044	Figure 5C
left superior temporal gyrus	-39	+21	-24	72	0.1170 ± 0.0024	0.1031 ± 0.0022	Figure 6
left superior temporal gyrus	-23	+9	-26	2	0.1718 ± 0.0038	0.1533 ± 0.0040	
inferior longitudinal fasciculus	-45	-41	+17	88	0.2785 ± 0.0033	0.2583 ± 0.0045	Figure 5B
superior temporal gyrus	-59	-39	+17	36	0.1769 ± 0.0031	0.1571 ± 0.0036	

appeared in the corticospinal tract, nearby pontine neurons, the middle cerebellar peduncle, and the cerebellar deep nuclei. In addition, a large area within the anterior cingulate cortex showed structural alterations, as did the underlying cingulum bundle and portions of the nearby corpus callosum. Finally, reduced axonal integrity was apparent in the ventral medial prefrontal cortex and other areas of frontal cortex. The nature of the pathology remains

unclear, but likely includes demyelination, shrinkage of axons, and axonal loss, and possibly lesions due to small vessel damage.

Comparison with Previous Neuroimaging Findings

The structural changes appeared in regions previously shown to be functionally or anatomically affected in OSA, and in fiber



pathways interconnecting those regions. The hippocampus, for example, earlier showed reduced volume^{15,16} and signs of injury¹⁷ as well as abnormal responses to a number of challenges⁹⁻¹¹; in the present study, major hippocampal input (cingulum bundle) and output (fornix) pathways showed compromised integrity. The cingulum bundle also relays information to and from the cingulate cortex, a region that has shown gray matter loss¹⁵ and functional changes.^{7,9-13} The parietal deep white matter shows both lower FA and metabolic changes,^{18,20} likely indicating fiber

alterations in that area. Such changes could compromise relaying of sensory information, possibly contributing to the reduced sensitivity to mechanical stimuli in the upper airway of OSA patients.⁴¹ A third region which shows differences in FA, gray matter volume, and function is the cerebellum, with FA reflecting structural changes primarily in the deep regions and peduncles, and gray matter volume reflecting tissue loss in the cerebellar cortex. Both deficits likely compromise cerebellar functions.

Changes identified by DTI are sensitive to different underlying pathologies, compared to earlier gray matter loss and spectroscopic findings. Whereas lower FA primarily represents axonal groups that are damaged, shrunken, or that have less myelin, reduced gray matter volume likely represents atrophy that is the end result of some injurious process, and spectroscopic changes represent a combination of cell death (specifically reduced cell density) and altered metabolic activity. We speculate that the large number of changes found in FA, relative to gray matter volume alterations, may result from the early stage of pathologic processes. These processes subsequently result in atrophy and cell death. However, this possibility can only be assessed with longitudinal studies.

Potential Mechanisms of Injury

At least some of the axonal alterations found in OSA likely result from the repeated intermittent hypoxia accompanying apneic events in the syndrome. Exposing animals to intermittent hypoxia to simulate conditions comparable to interrupted breathing events in OSA affects corpus callosal fibers,²⁴ and induces cellular injury in the hippocampus and anterior fornix, regions throughout the thalamus and basal forebrain, the brainstem, and frontal cortex,^{24,42} and in cerebellar Purkinje cells and deep nuclei.²³ The latter cerebellar damage may result from excitotoxic activation of climbing fibers to Purkinje neurons from the inferior olive.⁴³ Injury to Purkinje and deep nuclei cells would lead to axonal degeneration; fiber integrity, especially myelin integrity, depends on maintained cellular activity.⁴⁴ Similar processes may be operating in frontal cortex, insular, and hippocampal structures,^{27,45} and contribute to the structural changes found in OSA cases here.

The repeated deoxygenation/reoxygenation with apneic episodes leads to a number of potentially detrimental oxidative and inflammatory processes. Inflammatory markers are elevated in animal models⁴⁶ and human OSA subjects,^{47,48} and are associated with neurodegeneration.⁴⁹ Direct oxidative damage occurs across many brain regions in animal models of OSA.^{24,26} Axons may also be damaged by stress-related compounds associated with high baseline sympathetic tone or sleep deprivation in the syndrome.^{48,50} Over time, these effects could lead to the larger-scale changes found here.

Cerebral perfusion is chronically altered in OSA⁵¹ and reduced during apneic events,^{52,53} creating a potential for ischemic damage. A common comorbidity in OSA is hypertension, which is associated with small vessel disease and leads to tissue injury visible as white matter hyperintensities on T2-weighted MRI scans,⁵⁴ a finding in some OSA studies.⁵⁵ The damage likely includes a combination of axonal injury and gliosis, confirmed by the reduced metabolite ratios found with magnetic resonance spectroscopy.^{18,20} More recent studies show that DTI changes re-

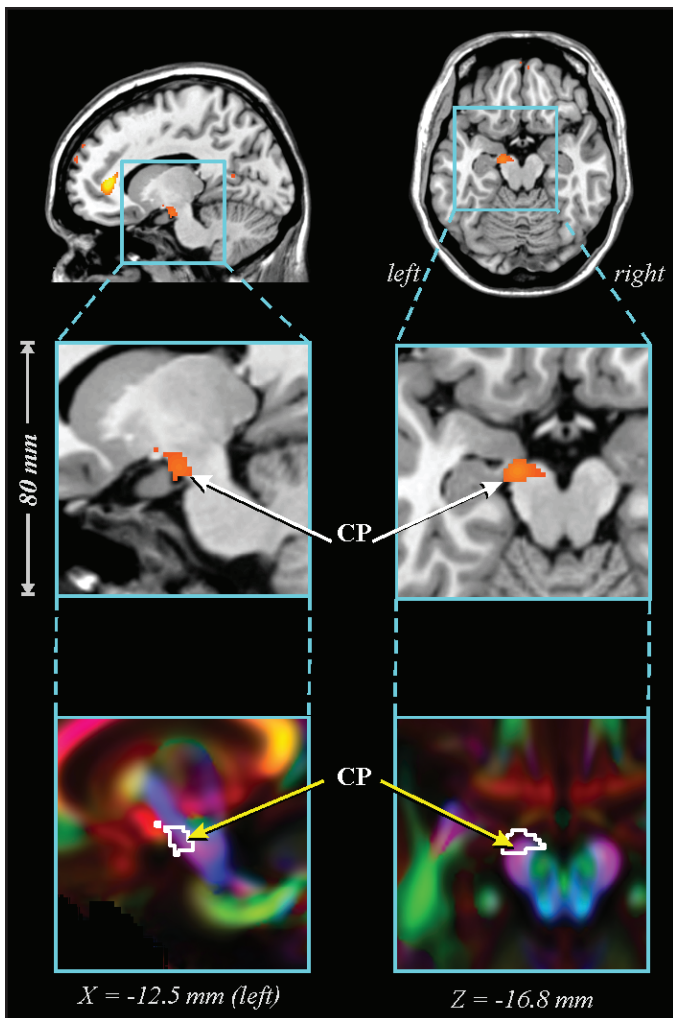


Figure 3—Lower FA in 41 OSA vs 69 control subjects in cerebral peduncle. CP: cerebral peduncle. See Figure 1 for key.

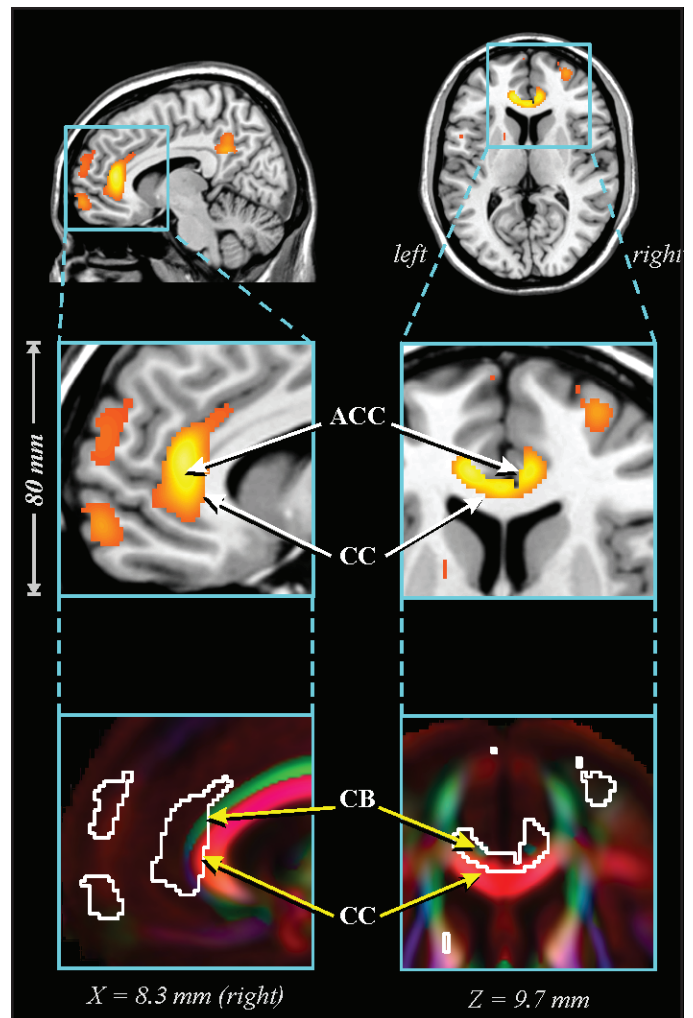


Figure 4—Lower FA in 41 OSA vs 69 control subjects in anterior cingulate area. ACC: anterior cingulate cortex; CB: superior-anterior cingulum bundle; CC: corpus callosum. See Figure 1 for key.

lated to small vessel disease largely correspond to axonal changes, rather than gliosis.⁵⁶ The presence of small lesions would lead to reduced FA as observed in the OSA subjects here.

A final possibility is that a portion of the brain structural changes preceded the onset of OSA. Although the mechanisms of injury expected to be operating with OSA (above) offer evidence that sleep apnea will lead to neuronal injury, MRI techniques cannot readily distinguish the source or timing of these neural changes. Thus, we can only speculate whether some of the structural changes resulted from an early insult, or maldevelopment. Brain changes can develop in subjects early in the disorder, including pediatric OSA subjects¹⁹ and recently diagnosed adult patients (present study), but the progressive nature of OSA means that by the time of diagnosis, most subjects have experienced months or years of the disorder. If prior injury is present, a further question is whether such alterations contribute to the onset of OSA, or to symptoms of the disorder.

Consequences for Behavior and Breathing

The affected structures have the potential to modify characteristics that are affected in OSA, including mood, cognition,

and cardiovascular regulation, as well as breathing control. However, while damage to cells in, and fiber pathways between, structures likely affects performance, the present study does not address how or when such damage arose.

Cardiovascular regulation would likely be affected by damage to the anterior cingulate cortex, ventral medial prefrontal cortex, amygdala, and cerebellar deep nuclei; all these structures are implicated in cardiovascular control.⁵⁷⁻⁶¹ Coordination and control of upper airway breathing musculature will be affected by the compromised integrity of the corticospinal tract, middle cerebellar peduncle, and deep cerebellar nuclei.⁶² The inadequate coordination of upper airway musculature with diaphragmatic action in OSA (suppression of upper airway musculature with diaphragmatic action when activation is required) likely results in part from deficits in a principal brain coordination area, the cerebellum, and the deep cerebellar nuclei, the output nuclei for the cerebellum, were found to be injured here.

The impaired cognitive performance shown by OSA patients may relate to structural changes in the anterior cingulate cortex and cingulum, hippocampus, fornix, cerebellum, and frontal cortex.⁶³ Damaged or reorganized fibers in frontal, cerebellar, and parietal regions have the potential to interfere with multiple

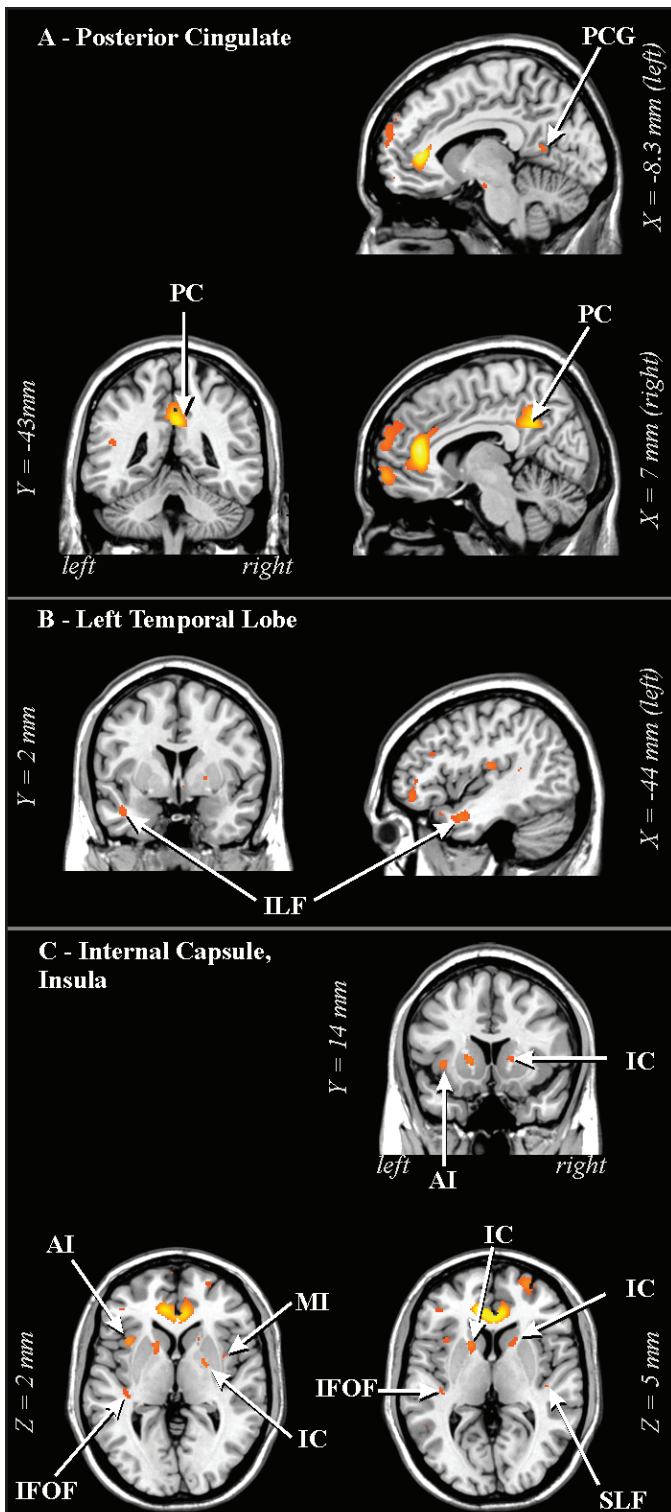


Figure 5—Lower FA in 41 OSA vs 69 control subjects in (A) posterior cingulate areas, (B) left temporal lobe, and (C) deep white matter and areas adjacent to the insula. AI: anterior insula; IFOF: inferior fronto-occipital fasciculus; ILF: inferior longitudinal fasciculus; MI: mid-insula; PC: posterior cingulate cortex/cingulum bundle; PCG: posterior cingulate gyrus; SLF: superior longitudinal fasciculus. See Figure 1 for key.

cognitive and behavioral aspects, including planning, hyperactive behaviors and spatial learning^{64,65}; deficits of this nature occur in OSA.^{66,67} Retention of cognitive deficiencies, even after

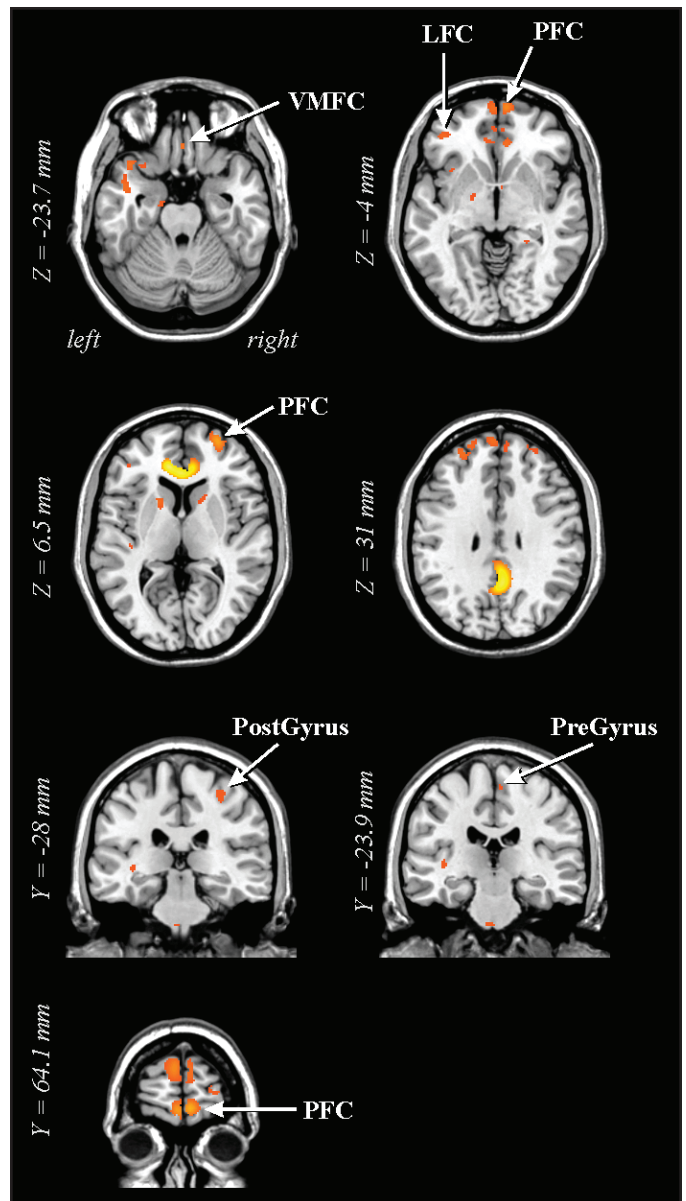


Figure 6—Lower FA in 41 OSA vs 69 control subjects in prefrontal regions and pre- and postcentral gyri. LFC: later frontal cortex; PFC: prefrontal cortex; PostGyrus: postcentral gyrus; PreGyrus: precentral gyrus; VMFC: ventral medial prefrontal cortex. See Figure 1 for key.

therapeutic intervention for the breathing disorder,⁵⁻⁷ is consistent with the presence of structural neural injury, which would not resolve from such ventilatory support.

Mood effects could stem from damage to limbic areas, i.e., the anterior cingulate and insula, and projections to the amygdala and hippocampus.⁶⁸ A number of axonal tracts interconnecting such structures were affected, including fibers of the fornix and the cingulum bundle; fibers in the ventral medial prefrontal cortex were also altered. The cingulum bundle sends projections to the hippocampus, insular cortex, and amygdala, and the fornix is a principal output path for the hippocampal formation. The affected limbic structures are instrumental in emotional expression. Fear and anxiety attributes depend on amygdala action, while insular regions are associated with dyspnea⁶⁹ and

other emotional aspects. An area extending from the genu of the anterior cingulate to the ventral medial prefrontal cortex participates in regulation of mood.^{60,70} Abnormalities in these limbic structures may contribute to the high incidence of depression and other mood disorders in OSA.⁷¹

These limbic structures also contribute substantially to autonomic regulation, affect, and memory processes through hypothalamic, brainstem and intermediate thalamic projections. The ventral medial prefrontal cortex modifies sympathetic outflow⁶⁰ as do portions of the cingulate cortex that send projections through the cingulum bundle.⁵⁷ The anterior insular cortex assists in baroreflex regulation,⁶¹ and both the hippocampus and amygdala play a role in blood pressure control.⁷² The structural changes likely compromise the normal function of these structures, contributing to the impaired autonomic control in OSA.

Most structures showed lowered FA bilaterally; however, in a number of areas, only unilateral changes appeared. We¹⁵ and others¹⁶ have earlier shown that neural alterations in OSA can appear principally on one side (e.g., hippocampus, anterior cingulate, frontal cortex). Lateralization of FA changes is of interest, since a one-sided expression suggests preferential perfusion deficits, a likely possibility considering the differential lateralization of the vascular supply to the brain.

Limitations

Limitations of this study include the restricted spatial resolution of the MRI technique and an inability to distinguish the precise nature of the abnormalities found. Spatial resolution is limited by both the MRI parameters and by the voxel-based group analysis, which requires normalizing each subject's brain volume to a common space. Because such normalization is not precise, the detected differences are only accurate to within a few millimeters, depending on the location within the brain and the extent of smoothing. Brainstem regions are more likely to be well-normalized than neo-cortical regions. However, structures in the brainstem tend to be smaller; thus, the net sensitivity of the technique across brain regions is unclear. The finite resolution of the MRI scanner also results in partial volume effects, i.e., measurement of FA at each voxel is an "average" property of the large number of neurons and fibers within that voxel. Confounding partial volume effects are especially likely in some brainstem regions containing multiple cellular groups and crossing fibers. A further consideration is that DTI images are prone to distortion in certain brain areas, in particular the ventral frontal cortex above the orbit. The fieldmap correction that was applied compensates for geometric distortions,³⁴ but high signal variance in ventral frontal regions remains.

The interpretation of neural changes represented by lower FA has a number of limitations. Structural changes as measured by FA are influenced by a number of factors including sex, age, and small vessel disease. The control group had a higher proportion of females, which may have slightly reduced group differences since females tend to have lower FA than males.⁷³ Age also influences FA, with most brain regions showing decreasing structural integrity with increasing age in adults;⁷⁴ we did include age as a covariate in the statistical analysis, but such an approach only removes linearly related age influences. Finally,

while we interpreted brain regions with lower FA as having reduced fiber integrity, we could not distinguish between reduced myelin and reduced numbers of axons; however, neural communication is affected in either circumstance.

Conclusions

Patients with OSA showed loss of fiber integrity in brain regions associated with behavioral and physiological functions that are deficient in OSA. The deficits appeared in multiple regions, and possibly reflect damage resulting from a number of processes, including hypoxia, oxidative stress, chronic inflammation, small vessel disease, and local ischemia. The structural changes likely represent accumulated injury over sustained periods of time, and presumably would not be immediately resolved with conventional therapeutic interventions for OSA. The findings suggest that future treatment for OSA might consider neuroprotective interventions to prevent neural injury.

ACKNOWLEDGMENTS

The authors thank Ms. Rebecca Harper, Dr. Stacy L. Serber, and Dr. Rebecca L. Cross for assistance with data collection. The studies were supported by HL-60296.

REFERENCES

1. Schroder CM, O'Hara R. Depression and obstructive sleep apnea (OSA). *Ann Gen Psychiatry* 2005;4:13.
2. Sateia MJ. Neuropsychological impairment and quality of life in obstructive sleep apnea. *Clin Chest Med* 2003;24:249-59.
3. Beebe DW, Groesz L, Wells C, Nichols A, McGee K. The neuropsychological effects of obstructive sleep apnea: a meta-analysis of norm-referenced and case-controlled data. *Sleep* 2003;26:298-307.
4. Cortelli P, Parchi P, Sforza E, et al. Cardiovascular autonomic dysfunction in normotensive awake subjects with obstructive sleep apnoea syndrome. *Clin Auton Res* 1994;4:57-62.
5. Ferini-Strambi L, Baietto C, Di Gioia MR, et al. Cognitive dysfunction in patients with obstructive sleep apnea (OSA): partial reversibility after continuous positive airway pressure (CPAP). *Brain Res Bull* 2003;61:87-92.
6. El-Ad B, Lavie P. Effect of sleep apnea on cognition and mood. *Int Rev Psychiatry* 2005;17:277-82.
7. Thomas RJ, Rosen BR, Stern CE, Weiss JW, Kwong KK. Functional imaging of working memory in obstructive sleep-disordered breathing. *J Appl Physiol* 2005;98:2226-34.
8. Carlson JT, Hedner J, Elam M, Ejnell H, Sellgren J, Wallin BG. Augmented resting sympathetic activity in awake patients with obstructive sleep apnea. *Chest* 1993;103:1763-8.
9. Henderson LA, Woo MA, Macey PM, et al. Neural responses during Valsalva maneuvers in obstructive sleep apnea syndrome. *J Appl Physiol* 2003;94:1063-74.
10. Macey KE, Macey PM, Woo MA, et al. Inspiratory loading elicits aberrant fMRI signal changes in obstructive sleep apnea. *Respiratory Physiol Neurobiol* 2006;151:44-60.
11. Harper RM, Macey PM, Henderson LA, et al. fMRI responses to cold pressor challenges in control and obstructive sleep apnea subjects. *J Appl Physiol* 2003;94:1583-95.
12. Ayalon L, Ancoli-Israel S, Klempfuss Z, Shalauta MD, Drummond SP. Increased brain activation during verbal learning in obstructive sleep apnea. *Neuroimage* 2006;31:1817-25.
13. Macey PM, Macey KE, Henderson LA, et al. Functional magnetic

- resonance imaging responses to expiratory loading in obstructive sleep apnea. *Respir Physiol Neurobiol* 2003;138:275-90.
14. Davies CW, Crosby JH, Mullins RL, et al. Case control study of cerebrovascular damage defined by magnetic resonance imaging in patients with OSA and normal matched control subjects. *Sleep* 2001;24:715-20.
 15. Macey PM, Henderson LA, Macey KE, et al. Brain morphology associated with obstructive sleep apnea. *Am J Respir Crit Care Med* 2002;166:1382-7.
 16. Morrell MJ, McRobbie DW, Quest RA, Cummin AR, Ghiassi R, Corfield DR. Changes in brain morphology associated with obstructive sleep apnea. *Sleep Med* 2003;4:451-4.
 17. Bartlett DJ, Rae C, Thompson CH, et al. Hippocampal area metabolites relate to severity and cognitive function in obstructive sleep apnea. *Sleep Med* 2004;5:593-6.
 18. Kamba M, Inoue Y, Higami S, Suto Y, Ogawa T, Chen W. Cerebral metabolic impairment in patients with obstructive sleep apnoea: an independent association of obstructive sleep apnoea with white matter change. *J Neurol Neurosurg Psychiatry* 2001;71:334-9.
 19. Halbower AC, Degaonkar M, Barker PB, et al. Childhood obstructive sleep apnea associates with neuropsychological deficits and neuronal brain injury. *PLoS medicine* 2006;3:e301.
 20. Tonon C, Vetrugno R, Lodi R, et al. Proton magnetic resonance spectroscopy study of brain metabolism in obstructive sleep apnoea syndrome before and after continuous positive airway pressure treatment. *Sleep* 2007;30:305-11.
 21. O'Donoghue FJ, Briellmann RS, Rochford PD, et al. Cerebral structural changes in severe obstructive sleep apnea. *Am J Respir Crit Care Med* 2005;171:1185-90.
 22. Macey PM, Harper RM. OSA brain morphology differences: magnitude of loss approximates age-related effects. *Am J Respir Crit Care Med* 2005;172:1056-7; author reply 7-8.
 23. Pae EK, Chien P, Harper RM. Intermittent hypoxia damages cerebellar cortex and deep nuclei. *Neurosci Lett* 2005;375:123-8.
 24. Veasey SC, Davis CW, Fenik P, et al. Long-term intermittent hypoxia in mice: protracted hypersomnolence with oxidative injury to sleep-wake brain regions. *Sleep* 2004;27:194-201.
 25. Xu W, Chi L, Row BW, et al. Increased oxidative stress is associated with chronic intermittent hypoxia-mediated brain cortical neuronal cell apoptosis in a mouse model of sleep apnea. *Neuroscience* 2004;126:313-23.
 26. Zhu Y, Fenik P, Zhan G, et al. Selective loss of catecholaminergic wake active neurons in a murine sleep apnea model. *J Neurosci* 2007;27:10060-71.
 27. Kanaan A, Farahani R, Douglas RM, Lamanna JC, Haddad GG. Effect of chronic continuous or intermittent hypoxia and reoxygenation on cerebral capillary density and myelination. *Am J Physiol Regul Integr Comp Physiol* 2006;290:R1105-14.
 28. Le Bihan D, Mangin JF, Poupon C, et al. Diffusion tensor imaging: concepts and applications. *J Magn Reson Imaging* 2001;13:534-46.
 29. Mac Donald CL, Dikranian K, Song SK, Bayly PV, Holtzman DM, Brody DL. Detection of traumatic axonal injury with diffusion tensor imaging in a mouse model of traumatic brain injury. *Exp Neurol* 2007;205:116-31.
 30. Burns J, Job D, Bastin ME, et al. Structural disconnectivity in schizophrenia: a diffusion tensor magnetic resonance imaging study. *Br J Psychiatry* 2003;182:439-43.
 31. Faul F, Erdfelder E, Lang AG, Buchner A. G*Power 3: a flexible statistical power analysis program for the social, behavioral, and biomedical sciences. *Behav Res Methods* 2007;39:175-91.
 32. Sleep-related breathing disorders in adults: recommendations for syndrome definition and measurement techniques in clinical research. The Report of an American Academy of Sleep Medicine Task Force. *Sleep* 1999;22:667-89.
 33. Knutson KL, Rathouz PJ, Yan LL, Liu K, Lauderdale DS. Stability of the Pittsburgh Sleep Quality Index and the Epworth Sleepiness Questionnaires over 1 year in early middle-aged adults: the CARDIA study. *Sleep* 2006;29:1503-6.
 34. Hutton C, Bork A, Josephs O, Deichmann R, Ashburner J, Turner R. Image distortion correction in fMRI: A quantitative evaluation. *Neuroimage* 2002;16:217-40.
 35. Friston KJ, Holmes AP, Poline JB, et al. Analysis of fMRI time-series revisited. *Neuroimage* 1995;2:45-53.
 36. Basser PJ, Pierpaoli C. Microstructural and physiological features of tissues elucidated by quantitative-diffusion-tensor MRI. *J Magn Reson B* 1996;111:209-19.
 37. Ashburner J, Friston KJ. Unified segmentation. *Neuroimage* 2005;26:839-51.
 38. Jones DK, Symms MR, Cercignani M, Howard RJ. The effect of filter size on VBM analyses of DT-MRI data. *Neuroimage* 2005;26:546-54.
 39. Pajevic S, Pierpaoli C. Color schemes to represent the orientation of anisotropic tissues from diffusion tensor data: application to white matter fiber tract mapping in the human brain. *Magn Reson Med* 1999;42:526-40.
 40. Alexander DC, Pierpaoli C, Basser PJ, Gee JC. Spatial transformations of diffusion tensor magnetic resonance images. *IEEE Trans Med Imaging* 2001;20:1131-9.
 41. Kimoff RJ, Sforza E, Champagne V, Ofiara L, Gendron D. Upper airway sensation in snoring and obstructive sleep apnea. *Am J Respir Crit Care Med* 2001;164:250-5.
 42. Gozal D, Daniel JM, Dohanich GP. Behavioral and anatomical correlates of chronic episodic hypoxia during sleep in the rat. *J Neurosci* 2001;21:2442-50.
 43. Welsh JP, Yuen G, Placantonakis DG, et al. Why do Purkinje cells die so easily after global brain ischemia? Aldolase C, EAAT4, and the cerebellar contribution to posthypoxic myoclonus. *Adv Neurol* 2002;89:331-59.
 44. Ishibashi T, Dakin KA, Stevens B, et al. Astrocytes promote myelination in response to electrical impulses. *Neuron* 2006;49:823-32.
 45. Moss I, An T, Krishnaswamy A, LaFerrière A. Intermittent hypoxia increases apoptosis in agranular insular cortex of neonatal rat. *FASEB J* 2004;18:A1059.
 46. Zhan G, Fenik P, Pratico D, Veasey SC. Inducible nitric oxide synthase in long-term intermittent hypoxia: hypersomnolence and brain injury. *Am J Respir Crit Care Med* 2005;171:1414-20.
 47. Ohga E, Tomita T, Wada H, Yamamoto H, Nagase T, Ouchi Y. Effects of obstructive sleep apnea on circulating ICAM-1, IL-8, and MCP-1. *J Appl Physiol* 2003;94:179-84.
 48. Shamsuzzaman AS, Winnicki M, Lanfranchi P, et al. Elevated C-reactive protein in patients with obstructive sleep apnea. *Circulation* 2002;105:2462-4.
 49. McLaurin J, D'Souza S, Stewart J, et al. Effect of tumor necrosis factor alpha and beta on human oligodendrocytes and neurons in culture. *Int J Dev Neurosci* 1995;13:369-81.
 50. Kokturk O, Ciftci TU, Mollarecep E, Ciftci B. Elevated C-reactive protein levels and increased cardiovascular risk in patients with obstructive sleep apnea syndrome. *Int Heart J* 2005;46:801-9.
 51. Ficker JH, Feistel H, Moller C, et al. [Changes in regional CNS perfusion in obstructive sleep apnea syndrome: initial SPECT studies with injected nocturnal 99mTc-HMPAO]. *Pneumologie* 1997;51:926-30.
 52. Balfors EM, Franklin KA. Impairment of cerebral perfusion during obstructive sleep apneas. *Am J Respir Crit Care Med* 1994;150(6 Pt 1):1587-91.
 53. Hayakawa T, Terashima M, Kayukawa Y, Ohta T, Okada T. Changes in cerebral oxygenation and hemodynamics during obstructive sleep apneas. *Chest* 1996;109:916-21.
 54. Fazekas F, Kleinert R, Offenbacher H, et al. Pathologic correlates

- of incidental MRI white matter signal hyperintensities. *Neurology* 1993;43:1683-9.
55. Aloia M, Arnedt J, Davis J, et al. MRI white matter hyperintensities in older adults with OSA. *Sleep* 2001;24:A55.
 56. Nitkunan A, Charlton RA, McIntyre DJ, Barrick TR, Howe FA, Markus HS. Diffusion tensor imaging and MR spectroscopy in hypertension and presumed cerebral small vessel disease. *Magn Reson Med* 2008 Jan 25 [epub ahead of print]
 57. Burns SM, Wyss JM. The involvement of the anterior cingulate cortex in blood pressure control. *Brain Res* 1985;340:71-7.
 58. Critchley HD, Corfield DR, Chandler MP, Mathias CJ, Dolan RJ. Cerebral correlates of autonomic cardiovascular arousal: a functional neuroimaging investigation in humans. *J Physiol* 2000;523 Pt 1:259-70.
 59. Kimmerly DS, O'Leary DD, Menon RS, Gati JS, Shoemaker JK. Cortical regions associated with autonomic cardiovascular regulation during lower body negative pressure in humans. *J Physiol* 2005;569(Pt 1):331-45.
 60. King AB, Menon RS, Hachinski V, Cechetto DF. Human forebrain activation by visceral stimuli. *J Comp Neurol* 1999;413:572-82.
 61. Zhang Z, Oppenheimer SM. Characterization, distribution and lateralization of baroreceptor-related neurons in the rat insular cortex. *Brain Res* 1997;760:243-50.
 62. Chen ML, Witmans MB, Tablizo MA, et al. Disordered respiratory control in children with partial cerebellar resections. *Pediatr Pulmonol* 2005;40:88-91.
 63. Bunge SA, Burrows B, Wagner AD. Prefrontal and hippocampal contributions to visual associative recognition: interactions between cognitive control and episodic retrieval. *Brain Cogn* 2004;56:141-52.
 64. Ridderinkhof KR, Ullsperger M, Crone EA, Nieuwenhuis S. The role of the medial frontal cortex in cognitive control. *Science* 2004;306:443-7.
 65. Schmithorst VJ, Wilke M, Dardzinski BJ, Holland SK. Cognitive functions correlate with white matter architecture in a normal pediatric population: a diffusion tensor MRI study. *Hum Brain Mapp* 2005;26:139-47.
 66. Beebe DW, Wells CT, Jeffries J, Chini B, Kalra M, Amin R. Neuropsychological effects of pediatric obstructive sleep apnea. *J Int Neuropsychol Soc* 2004;10:962-75.
 67. Engleman H, Joffe D. Neuropsychological function in obstructive sleep apnoea. *Sleep Med Rev* 1999;3:59-78.
 68. Hastings RS, Parsey RV, Oquendo MA, Arango V, Mann JJ. Volumetric analysis of the prefrontal cortex, amygdala, and hippocampus in major depression. *Neuropsychopharmacology* 2004;29:952-9.
 69. Peiffer C, Poline JB, Thivard L, Aubier M, Samson Y. Neural substrates for the perception of acutely induced dyspnea. *Am J Respir Crit Care Med* 2001;163:951-7.
 70. Drevets WC, Price JL, Simpson JR Jr, et al. Subgenual prefrontal cortex abnormalities in mood disorders. *Nature* 1997;386:824-7.
 71. Reynolds CF 3rd, Kupfer DJ, McEachran AB, Taska LS, Sewitch DE, Coble PA. Depressive psychopathology in male sleep apneics. *J Clin Psychiatry* 1984;45:287-90.
 72. Dietl H. Differential effects of experimentally induced blood pressure changes on the release of catecholamines in hypothalamic and limbic areas of rats. *Life Sci* 1987;41:217-26.
 73. Huster RJ, Westerhausen R, Kreuder F, Schweiger E, Wittling W. Hemispheric and gender related differences in the midcingulum bundle: A DTI study. *Hum Brain Mapp* 2007 Dec 6 [epub ahead of print]
 74. Pfefferbaum A, Sullivan EV, Hedehus M, Lim KO, Adalsteinsson E, Moseley M. Age-related decline in brain white matter anisotropy measured with spatially corrected echo-planar diffusion tensor imaging. *Magn Reson Med* 2000;44:259-68.